NASA TECHNICAL NOTE

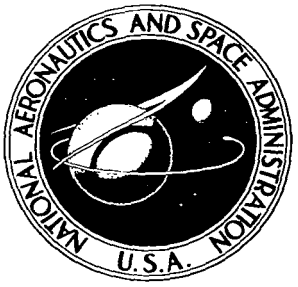

NASA TN D-2015

NASA TN D-2015

INVESTIGATION OF THE CALORIMETRIC EFFICIENCY OF A SPLIT-RIB UMBRELLA-TYPE PARABOLOIDAL SOLAR ENERGY CONCENTRATOR

by John D. Camp and William D. Nowlin

Langley Research Center
Langley Station, Hampton, Va.

NATIONAL AERONAUTICS AND SPACE ADMINISTRATION • WASHINGTON, D. C. • MARCH 1964

INVESTIGATION OF THE CALORIMETRIC EFFICIENCY OF A SPLIT-RIB UMBRELLA-TYPE PARABOLOIDAL SOLAR ENERGY CONCENTRATOR

By John D. Camp and William D. Nowlin

Langley Research Center
Langley Station, Hampton, Va.

NATIONAL AERONAUTICS AND SPACE ADMINISTRATION

For sale by the Office of Technical Services, Department of Commerce,
Washington, D.C. 20230 -- Price $0.75

INVESTIGATION OF THE CALORIMETRIC EFFICIENCY OF A SPLIT-RIB UMBRELLA-TYPE PARABOLOIDAL SOLAR ENERGY CONCENTRATOR

By John D. Camp and William D. Nowlin

SUMMARY

An investigation of the calorimetric efficiency of a 10-foot-diameter split-rib umbrella-type paraboloidal solar energy concentrator was performed. The method of fabricating this concentrator from a previously existing 60-rib umbrella-type concentrator is discussed. The split-rib configuration is illustrated and some aspects of the design and construction of the spherical-type calorimeters are discussed.

Calorimetric tests were performed, employing three spherical calorimeters with 3-inch, 6.25-inch, and 12-inch diameters. The variation in the geometrical efficiency with the diameter ratio is shown and comparison with the previously tested 60-rib concentrator is made. Maximum geometrical efficiencies obtained were 100, 81, and 40 percent with the 12-inch-, 6.25-inch-, and 3-inch-diameter calorimeters, respectively. The experimentally obtained efficiencies are compared with theoretical values.

This investigation has demonstrated that attempts to improve the efficiency of an umbrella-type concentrator by increasing the number of ribs without significantly decreasing the stress-geometry parameter result in improvements which are small in comparison to what could be effected by reducing the stress-geometry parameter.

INTRODUCTION

Solar energy concentrators employing reflective surfaces with a paraboloidal geometry have been investigated by a number of research organizations active in the area of auxiliary space power systems (ref. 1). Such concentrators are designed to intercept and concentrate the solar electromagnetic radiation available in space and to provide the necessary temperatures and heat inputs to operate conversion apparatus such as turbogenerators and thermoelectric and thermionic converters. Variations in the methods of fabricating concentrators and the choice of basic structural materials are due primarily to the influence of such factors as the required power output, type of energy-conversion components, weight and payload packaging restrictions, and the desired concentrator efficiency.

The basic structural elements of a solar concentrator are the reflector face, the reflective surface coating, and the backing structure. The reflective surface coating is applied to the front surface or face of the concentrator in order to obtain a high specular reflectance. The reflector face is generally made of a thin rigid or pliable skin of metal or plastic which is mounted on or attached to the backing structure. The concentrator is fabricated in such a manner that the reflector-face material or the backing structure, or both, may act as the shape-determining structural elements to achieve the desired configuration. The types of concentrators under development differ as to their relative structural rigidity and the methods of deployment and maintenance of the paraboloidal shape. In general, they may be grouped into four categories designated as rigid, nonrigid, semirigid, and rigidized (ref. 2).

The rigid type of concentrator may be of single-unit construction or may consist of segmented panels which may be furlable for packaging and deployment. In either case, the reflector structural elements cannot be bent or folded without damage to the concentrator. The nonrigid, semirigid, and rigidized types are similar in that all employ a thin pliable film as a reflector face, but differ in the manner in which the film is supported. Essentially, the nonrigid type has no backing structure other than the reflector film itself, and it employs a uniform force field such as gas pressure or centrifugal force to stress the skin to the paraboloidal configuration. The rigidized type is deployed in the same manner as the nonrigid concentrator and a rigid backing structure is formed after the deployment in space by using plastic foam or some other hardening agent. In the semirigid type of structure, the reflector face or skin material is supported at discrete lines or points by relatively rigid backing elements.

There are various problems associated with each of the above types of concentrators. Investigations thus far seem to indicate that only the rigid type of structure is capable of the high degree of geometrical accuracy required for such high-temperature applications as thermionic systems. However, it is possible that with further development and a more careful design, a nonrigid, semirigid, or rigidized type of concentrator can be constructed that will be suitable for a high-temperature system. The advantages of these types are that they are generally lighter, can be folded and packaged in a smaller volume, and can therefore be made larger than the rigid type. At the present state of development they are suitable for the lower temperatures as required by the thermoelectric- and turbogenerator-type conversion systems.

Research in the solar concentrator area has been conducted at the Langley Research Center along the lines of the semirigid concept, employing a simple umbrella type of construction. The results of an investigation of a 60-rib mechanically erectable umbrella-type concentrator employing tapered aluminum ribs with an aluminized Mylar reflective surface have been reported in reference 3. In this type of structure the reflective membrane is attached to the ribs so as to exert the necessary bending moments to pull the ribs into a parabolic shape. The tension in the membrane is sufficient to remove the wrinkles and to form smooth flat reflecting segments between the ribs. It is apparent that there are inherent geometric errors in such a concentrator due to the flat segments between the ribs. The desired paraboloidal geometry can be more closely approached by increasing the number of ribs and hence reducing the width of these flat segments as much as possible. The results of the tests performed on the

60-rib concentrator indicated that it would be desirable to improve the surface geometry by increasing the number of ribs. A modification in the construction of the 60-rib concentrator was performed by splitting each rib in half from the tip of the rib down to a point chosen so that in the erected position the number of ribs was effectively doubled over approximately 80 percent of the projected frontal area of the concentrator. Calorimetric tests were performed on the split-rib concentrator and data are presented and compared herein with the performance of the previous model.

SYMBOLS

A	area, sq ft
c_v	specific heat, Btu/lb-$^{\circ}$R
d	calorimeter diameter, ft
D	concentrator diameter, ft
K	stress-geometry parameter
w	mass flow rate, lb/hr
Q	heat flux, Btu/hr
Q_S	total energy available from sun, $A_c Q_i$, Btu/hr
T	temperature, $^{\circ}$R
α	absorptance
γ	reflectance
ϵ	emittance
η	efficiency
σ	stress, lb/sq in.

Subscripts:

b	calorimeter
c	concentrator
g	geometrical
i	incident

s	meridional direction
s'	circumferential direction
u	usable
1	in
2	out

DESCRIPTION OF TEST CONCENTRATOR

The test concentrator was a modified 60-rib umbrella-type paraboloidal solar concentrator. The ribs of the previously tested 60-rib concentrator were split so that each rib effectively became two ribs from a radius of 26.4 inches from the optical axis out to the periphery of the concentrator. A new reflector surface of 1/2-mil Mylar with approximately 2,000 angstroms of vapor-deposited aluminum was laid on a plastic parabolic mold. The ribs were then bonded to the back side of the reflector surface, with the ribs being parted as shown in the sketch in figure 1. The split section of the ribs was spread to form a smooth curve until the ends were about 4 inches apart. This was done to keep the folded concentrator from having any abrupt bends which could be bent out of shape in the packaged condition. The actual shape of the rib configuration can be seen in the photographs shown as figures 2 and 3.

As was mentioned previously, the width of the flat segments is quite important since a beam of light reflected from such a segment will have a width equal to the width of the flat. It is therefore necessary to have a heat receiver or calorimeter which is no smaller than the maximum flat width if it is to be capable of intercepting all the radiation reflected from the concentrator.

The variation in the width of the flats with the distance from the optical axis of the concentrator is shown in figure 4. The dashed portion of the curve near the origin is due to the fact that the rib housing extends to a radius of 6.25 inches. As can be seen from the figure, the flat width for the split-rib concentrator follows that of the 60-rib concentrator to a radius of 26.4 inches. At this radius the ribs of the 60-rib concentrator, whose variation in flat width is represented by the dashed curve in figure 4, were split forming two flat-width portions which varied as shown by the solid curves in figure 4. The flat width on one of the portions increased from approximately 2.75 inches at a radius of 26.4 inches to a maximum of 3.5 inches at a radius of 43 inches and then decreased to 2.3 inches at the concentrator rim while the other flat portion increased from 0.0 inch at a radius of 26.4 inches to a maximum width of 4.0 inches at the concentrator rim.

The concentrator folds much the same as a common umbrella with the ribs folding forward to form a slightly tapered tube 6 feet long and $12\frac{1}{2}$ inches in diameter where the ribs join the hub. The concentrator is shown in the folded position in figure 5. Details of the erection mechanism are given in reference 3.

APPARATUS AND TEST PROCEDURE

The calorimetric efficiency tests of the 10-foot-diameter split-rib concentrator were conducted in a closed shed which was constructed for the purpose of testing in the presence of the actual sun and which provides protection from winds which would adversely affect the test results obtained for lightweight flexible structures. (See ref. 3 for photographs and detailed description.)

All the calorimetric efficiency tests which were performed were cold calorimeter tests employing spherical calorimeters which operate with a wall temperature slightly above the temperature of the surrounding air so that the effects of reradiation and convection can be ignored. The concentrator was mounted on an equatorial mounting with an electric clock drive for maintaining alinement with the sun. The alinement is originally set by observing the sun through an elbow telescope mounted parallel to the theoretical optical axis of the concentrator near the hub and is continually monitored during the tests. The calorimeter is a hollow sphere mounted on the end of two concentric tubes, and the tubes pass through the concentrator at the hub. A cross-sectional drawing of the 6.25-inch-diameter calorimeter is shown in figure 6. The hemispherical wedge inside the spherical calorimeter is used to channel the calorimetric fluid along the inside of the calorimeter wall. Figure 7 is a photograph of the cutaway sections of the 6.25-inch-diameter calorimeter and shows the internal construction. Water is pumped through the outside tube, forced against the inner surface of the sphere, and flows out through the inner tube. The rise in temperature of the water is measured by a system of differential thermocouples mounted in the inlet and outlet tubes.

The experimental setup for determining the calorimetric efficiency is illustrated schematically in figure 8. The amount of incident solar energy is determined by use of a normal incidence pyrheliometer mounted on the longitudinal axis of the mount. The mass flow rate of the water is measured with a turbine flow meter located in the inlet water line. The flow rate, differential temperature, and amount of incident solar energy are used to determine the overall efficiency of the collector by use of the following relation:

$$\eta = \frac{c_v w \Delta T}{A_c Q_i}$$

The differential temperature ΔT is kept low so that convection and radiation losses can be ignored, and the inlet water temperature is kept at the same temperature as the surrounding air or slightly lower. The geometrical efficiency of the concentrator can be obtained by dividing the overall efficiency by the solar reflectance of the reflector surface and the solar absorptance of the calorimeter. The geometrical efficiency can be expressed as

$$\eta_g = \frac{\eta}{\gamma_c \alpha_b}$$

A solar-reflectance value of 0.83 for the concentrator surface, used for efficiency calculations, was obtained from reference 3.

Tests were conducted by using three calorimeters having diameters of 3 inches, 6.25 inches, and 12 inches. Each calorimeter was positioned at various points along the optical axis to determine an experimental focal point.

RESULTS AND DISCUSSION

The theoretical focal length of the split-rib concentrator is 30 inches. However, because of geometrical imperfections in the actual concentrator surface and the spherical type of calorimeters which were used, an effective focal point along the optical axis at which the geometrical efficiency is a maximum must be determined experimentally for each calorimeter. The point referred to is the measured distance along the optical axis from the vertex of the paraboloid to the center of the spherical calorimeter. The effective focal point for each calorimeter is therefore determined by moving the calorimeter along the optical axis and determining the efficiency at various points until a point of maximum efficiency is located.

The graph in figure 9 illustrates the variation in geometrical efficiency as the calorimeter is moved along the optical axis. The maximum geometrical efficiences obtained were 40, 81, and 100 percent with the 3-inch-, 6.25-inch-, and 12-inch-diameter calorimeters, respectively. It can also be seen from figure 9 that the maximum geometrical efficiency is obtained over a small distance interval along the optical axis rather than at a single point. The maximum efficiency with the 12-inch-diameter calorimeter apparently occurred when the calorimeter was forward of the focal point as determined by the other two calorimeters. This was due to an error in the construction of the calorimeter and is explained in reference 3.

Perhaps it should be emphasized here that the geometrical efficiency as it has been defined and used herein depends upon the geometry and design of both the concentrating mirror and the calorimeter. Then a geometrical efficiency of 100 percent does not imply that the concentrator itself is geometrically perfect, but it indicates that with the particular concentrator-calorimeter system the maximum amount of intercepted solar energy is being collected, taking into account losses due to the reflectance of the concentrator and absorptance of the calorimeter.

A good measure of the accuracy of the surface geometry of the concentrator is its ability to concentrate the reflected solar radiation within a small region in the focal plane. This is indicated in figure 10 by a semilog graph of the variation in geometrical efficiency with the diameter ratio (the square of the ratio of the collector diameter to the calorimeter diameter). The plotted points represent the diameter ratios for the three different calorimeters which were employed. Figure 10 shows the noticeable improvement of the split-rib concentrator over the previously tested 60-rib model, but the geometrical efficiency still tends to decrease rapidly as the diameter ratio is increased.

A curve showing the theoretical geometrical efficiencies which should be attained with the split-rib concentrator for various size calorimeters is shown

in figure 11 along with the experimentally obtained curve. The theoretical values were obtained by assuming that the reflecting surfaces between ribs were perfectly flat segments and that the spherical calorimeter would intercept all radiation reflected from those areas of the concentrator where the flat width was less than or equal to the diameter of the calorimeter and would fail to intercept a calculated fraction of the radiation reflected from those areas when the flat width exceeded the diameter of the calorimeter. These areas were determined by graphical integration using a projected view similar to figure 1. It can be seen from the theoretical curve that the geometrical efficiency should increase with increasing calorimeter diameter until a geometrical efficiency of 100 percent is reached at a calorimeter diameter of 4 inches, which is also the maximum flat width of the split-rib concentrator. (See fig. 4.) The experimental curve shows that the actual concentrator does not reach a geometrical efficiency of 100 percent until the calorimeter diameter is about 12 inches.

The large spread between the theoretical and experimental values indicates that the reflecting surfaces between the ribs of the concentrator deviate from perfect flatness to such an extent that the performance of the concentrator is considerably degraded. The effects of distortions in the concentrator surface on the efficiencies of umbrella-type solar concentrators have been previously investigated both experimentally and theoretically and the results are reported in reference 4. It was concluded therein that the meridional tensions which are introduced when applying the reflecting membrane to the ribs for the purpose of eliminating wrinkles that develop transverse to the ribs, cause a distortion toward the axis of symmetry of the approximate paraboloid. This inward "bowing effect" on the reflecting surfaces between the ribs causes a dispersion of light rays in the theoretical focal plane of the concentrator with a resulting loss in concentrating ability.

The distortions in the concentrator surface and the consequent degradation in the geometrical efficiency can be related to a stress-geometry parameter which is dependent upon the ratio of the maximum stress in the meridional direction to the stress in the circumferential direction. It is also dependent upon the geometry of the umbrella concentrator or, more specifically, upon the ratio of the radius to the focal length. For the concentrator having a 90° rim angle (the angle subtended by the radius of the concentrator rim as seen from the focal point), the stress-geometry parameter can be shown to be (see ref. 4)

$$K = 0.556 \frac{\sigma_{s,max}}{\sigma_s'}$$

where K is the stress parameter, $\sigma_{s,max}$ is the maximum stress which occurs in the reflecting membrane in the meridional direction, and σ_s' is the stress in the membrane in the circumferential direction.

The variation of the geometrical efficiency with the diameter of the spherical calorimeter for various values of the stress-geometry parameter K is shown in figure 12. These curves are for a 60-rib concentrator with a 90° rim angle and are taken from data in reference 4. It can be seen from this figure that

with $K = 0$ a geometrical efficiency of 100 percent is obtained with a calorimeter diameter of about 6.28 inches, which is also the maximum flat width for a 60-rib 10-foot-diameter concentrator. As the stress-geometry parameter is increased, distortion of the surface takes place and it is evident from the curves with $K = 2$ and $K = 4$ that for any fixed calorimeter size the geometrical efficiency decreases considerably with increasing stress parameter.

The experimentally obtained curve showing the variation of the geometrical efficiency of the 60-rib concentrator with the calorimeter diameter is included on the graph of figure 12 for comparison with the theoretical curves of different values of K. The experimental curve for the 60-rib model indicates that the stress-geometry parameter for this concentrator lies somewhere between $K = 2$ and $K = 4$. The experimental curve for the split-rib model is also included in this figure for the purpose of showing that the improvement achieved by splitting the ribs was actually small in comparison with what could be attained with the 60-rib model if some method of reducing the stress-geometry parameter alone were possible without splitting the ribs.

A method of illustrating the temperature capabilities of a solar concentrator is to show the variation with temperature of the ratio of the energy removed from the calorimeter or heat receiver to the total energy available from the sun Q_u/A_cQ_i for various diameter ratios. This is shown in figure 13 for both the 60-rib and the split-rib concentrators. Again there is a noticeable improvement of the split-rib concentrator over the 60-rib model, but the limitations on the obtainable temperatures are still quite evident. At the higher temperatures the percentage of the available energy which can be extracted from the system is quite low.

A similar plot is shown in figure 14 where the three curves plotted are for the 3-inch-diameter calorimeter. This allows a comparison of the experimentally obtained curves for the 60-rib and split-rib concentrators and the theoretical curve for the split-rib concentrator at a fixed diameter ratio. For the theoretical curve, a geometrical efficiency of 0.96 is assumed for a 3-inch calorimeter as opposed to the experimental value of 0.407 (see fig. 11). As explained previously, the theoretical curves are based on the assumption of perfect flats corresponding to the stress-geometry-parameter value approaching zero.

CONCLUDING REMARKS

Calorimetric tests of the split-rib umbrella-type concentrator showed some degree of improvement over the 60-rib model. However, comparison of the experimental geometrical efficiencies with theoretical values and correlation with the results of data reported in NASA TN D-925 indicate that distortions of the concentrator surface due to an improper value of the stress-geometry parameter are present and result in losses in efficiency. This investigation has demonstrated that attempts to improve the efficiency of an umbrella-type concentrator by increasing the number of ribs without significantly decreasing the stress-geometry parameter result in improvements which are small in comparison to what could be effected by reducing the stress-geometry parameter. Problems related

to reducing the stress-geometry parameter do not appear incapable of solution. Significant improvements will be effected if future design work is directed toward an optimization of both the number of ribs and the stress-geometry parameters.

Langley Research Center,
National Aeronautics and Space Administration,
Langley Station, Hampton, Va., October 23, 1963.

REFERENCES

1. Heath, Atwood R., Jr.: Status of Solar Energy Collector Technology. [Preprint] 2531-62, American Rocket Soc., Sept. 1962.

2. McClelland, D. H., and Stephens, C. W.: Energy Conversion Systems Reference Handbook. Volume II - Solar-Thermal Energy Sources. WADD Tech. Rep. 60-699, Vol. II, U.S. Air Force, Sept. 1960. (Available from ASTIA as AD 256973.)

3. Nowlin, William D., and Benson, Harold E.: Study of Umbrella-Type Erectable Paraboloidal Solar Concentrators for Generation of Spacecraft Auxiliary Power. NASA TN D-1368, 1962.

4. Bond, Victor R.: Measurements and Calculations of the Effects of Distortions in the Collector Surface on Efficiencies of Umbrella-Type Solar Collectors. NASA TN D-925, 1961.

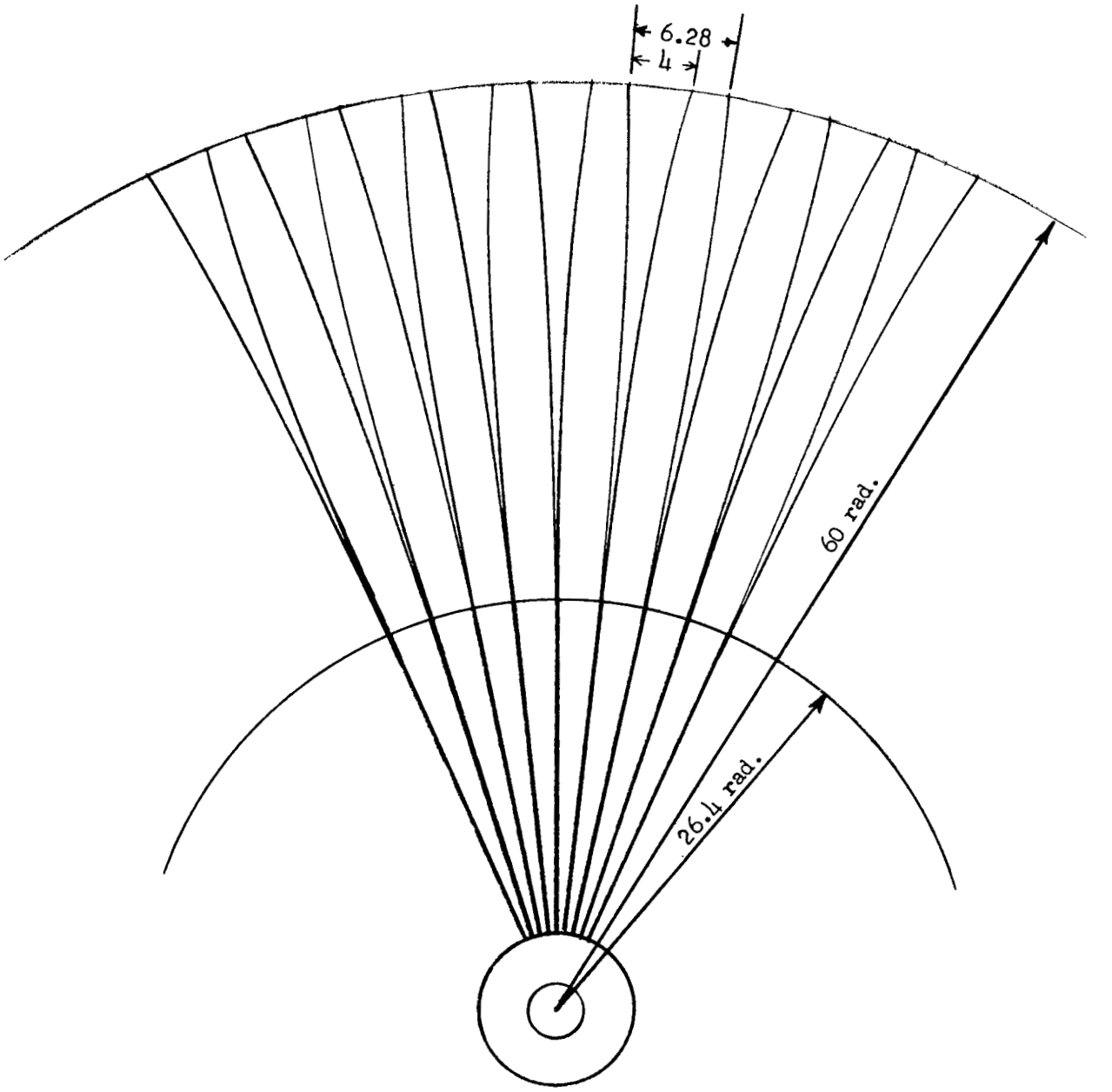

Figure 1.- Sketch showing rib layout for split-rib concentrator.
All dimensions are in inches.

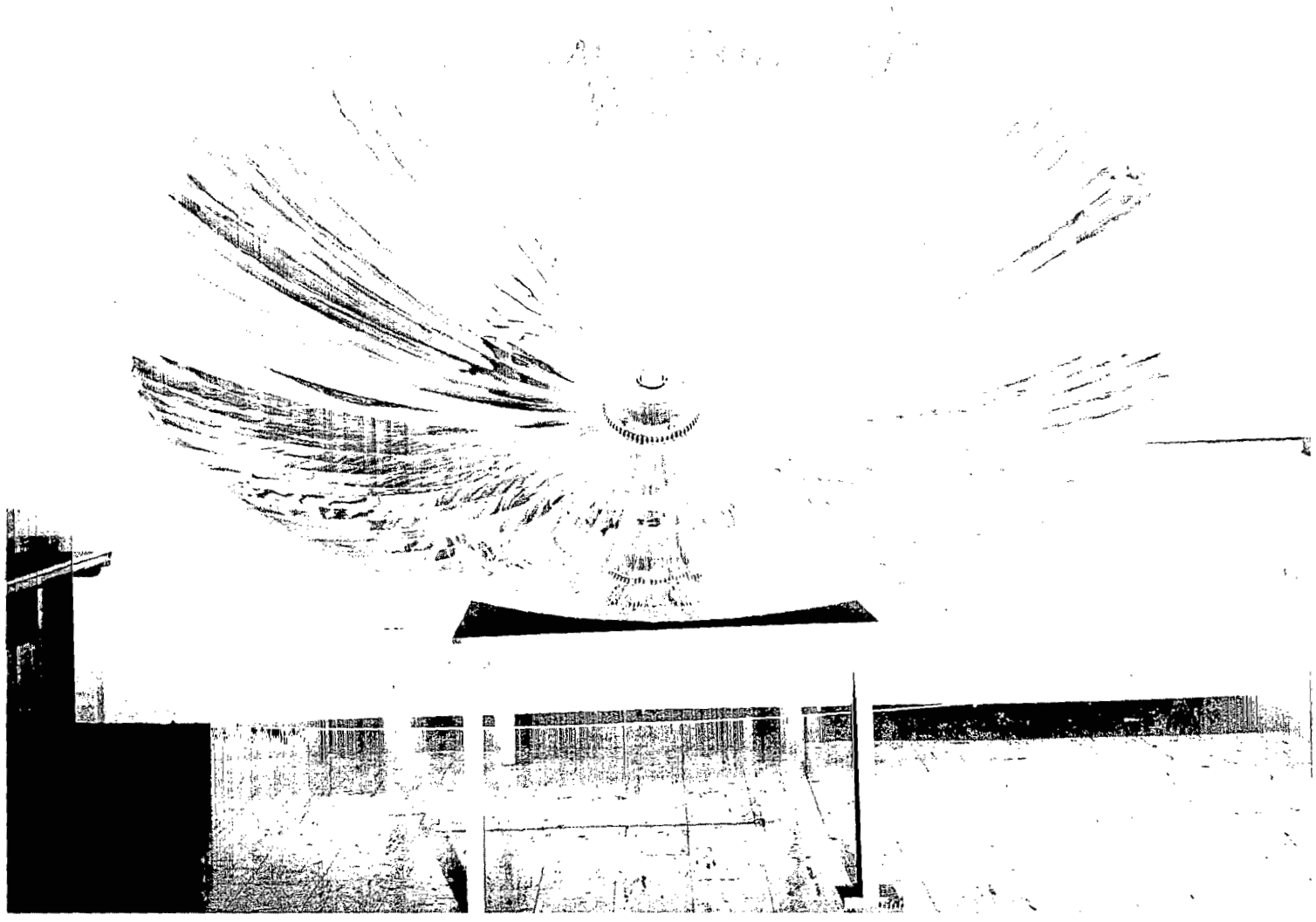

Figure 2.- 10-foot-diameter split-rib solar energy concentrator. L-62-7417

Figure 3.- Side view of 10-foot-diameter split-rib solar energy concentrator, showing rib arrangement. L-62-7419

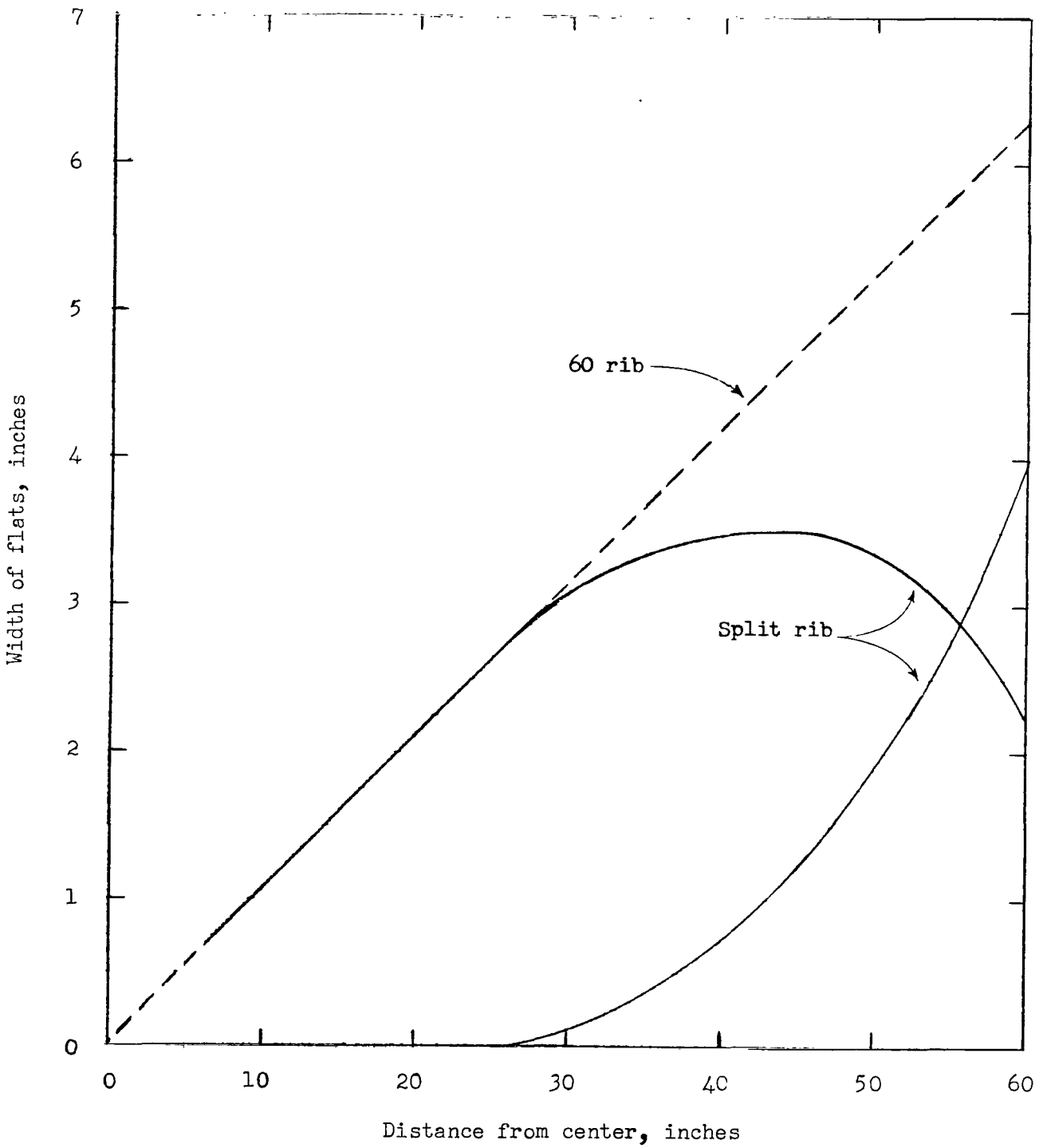

Figure 4.- Variation of width of flats with distance from center of concentrator for the 60-rib concentrator and the split-rib concentrator.

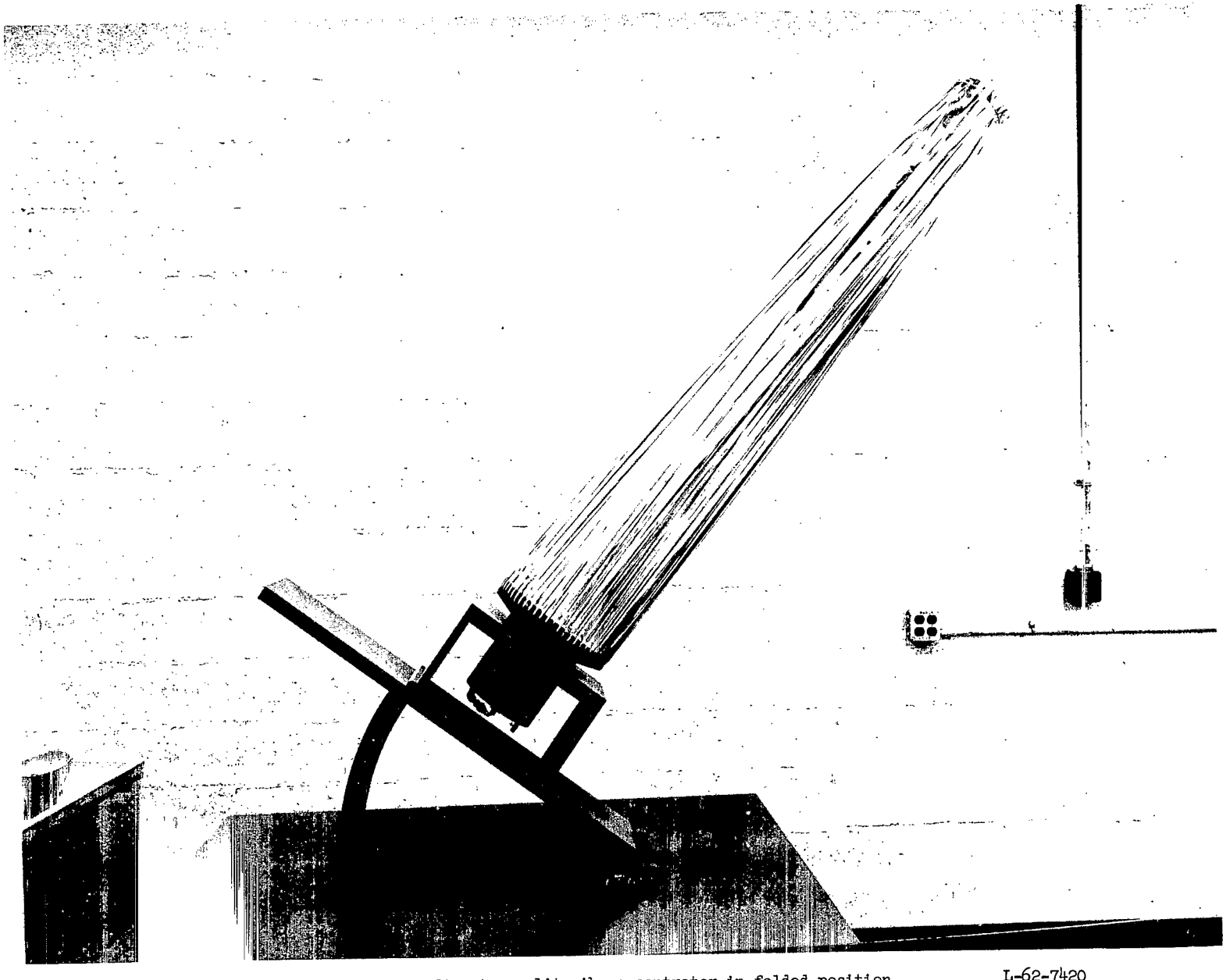

Figure 5.- 10-foot-diameter split-rib concentrator in folded position. L-62-7420

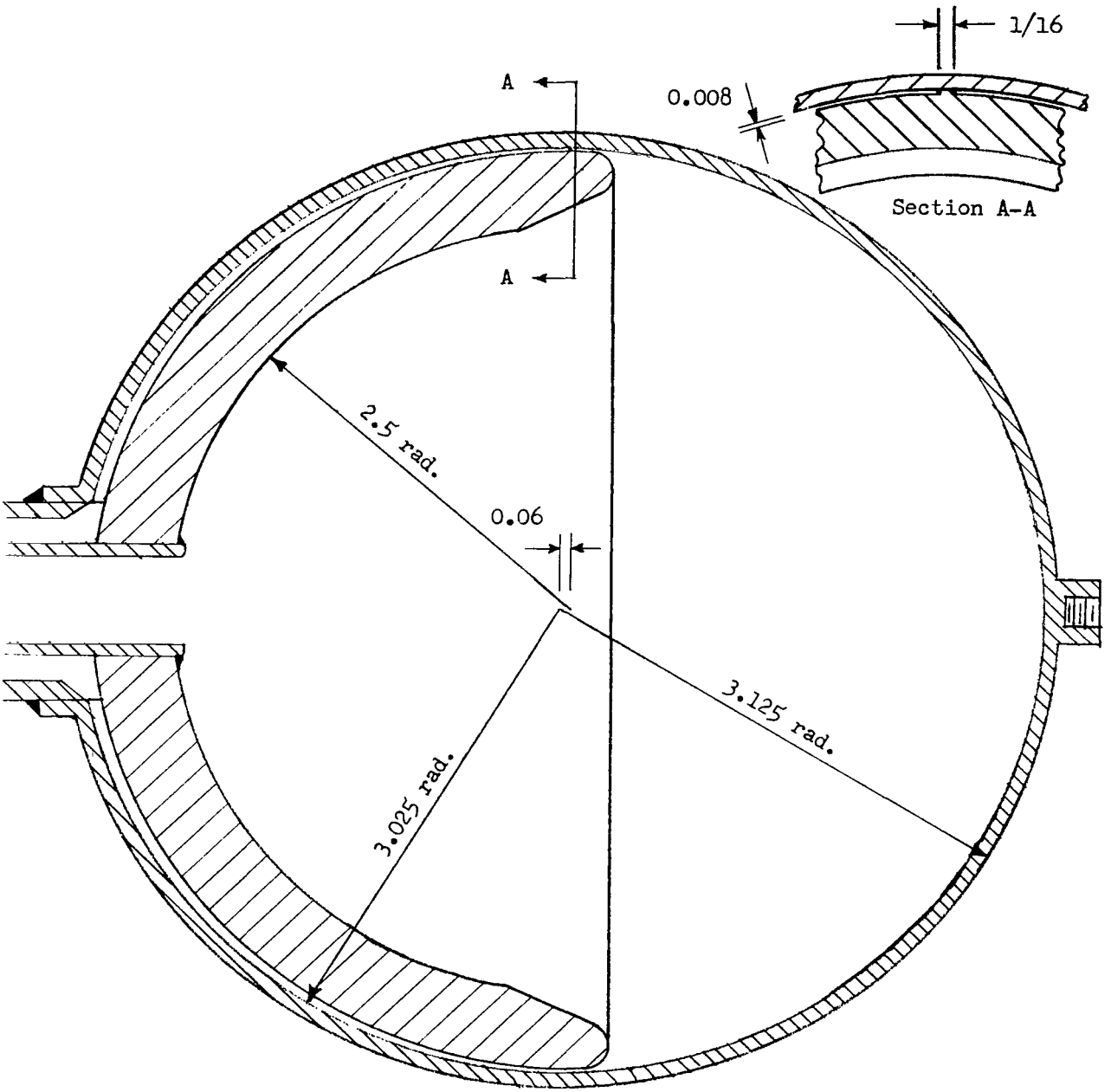

Figure 6.- Design for 6.25-inch-diameter calorimeter. All dimensions are in inches.

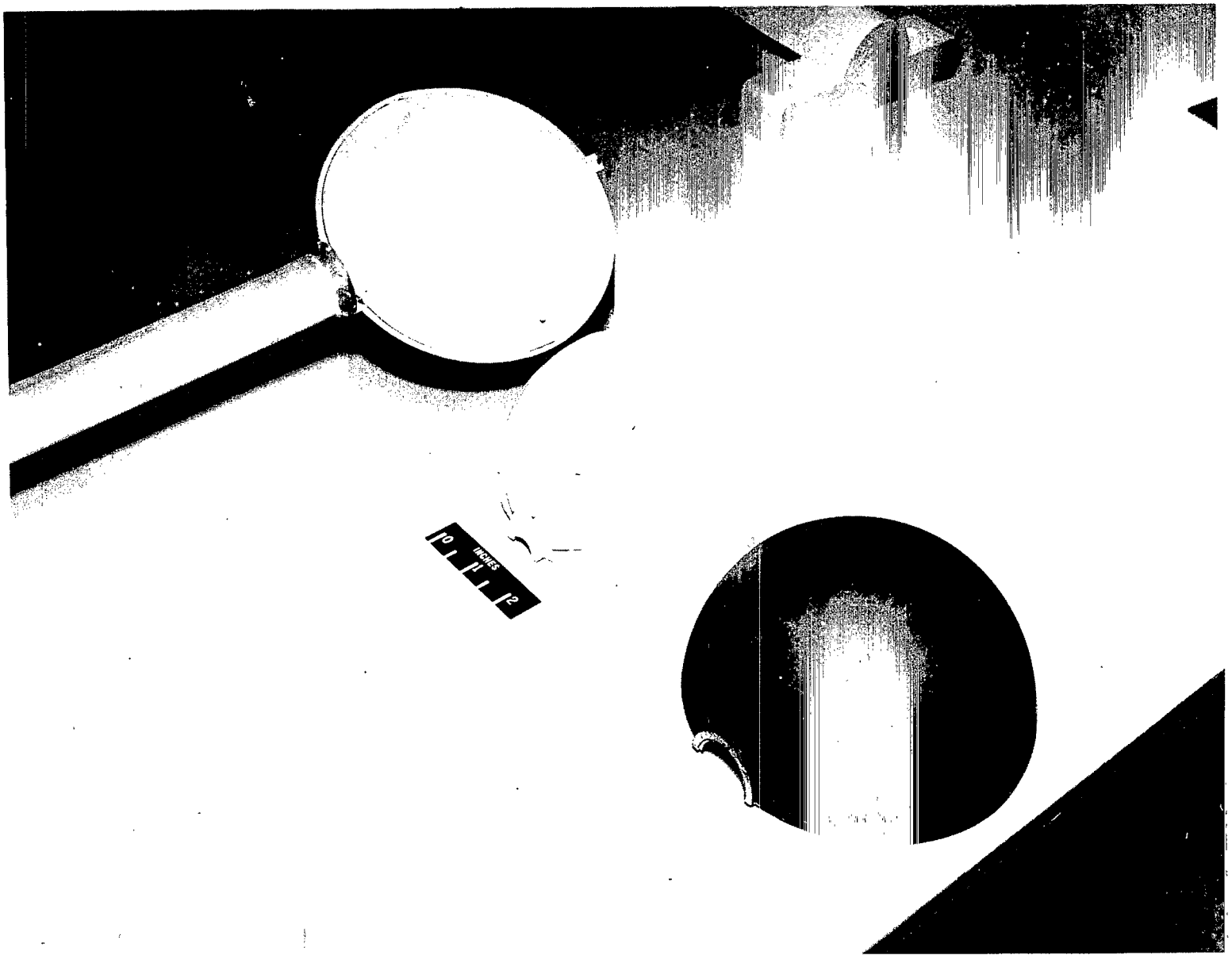

Figure 7.- Cutaway sections of 6.25-inch-diameter spherical calorimeter. L-62-7418

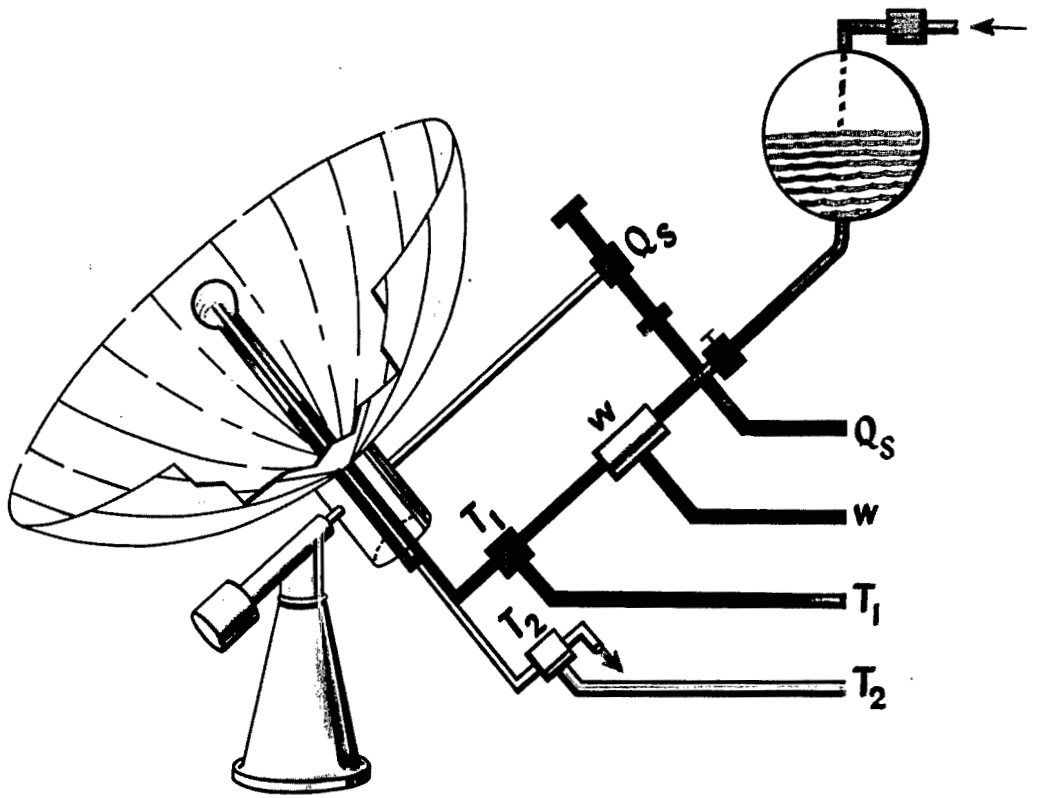

$$\text{EFFICIENCY} = \frac{Q_c}{Q_s} = \frac{(T_2 - T_1)wc_v}{Q_s}$$

Figure 8.- Schematic diagram of test setup for determination of calorimetric efficiency.

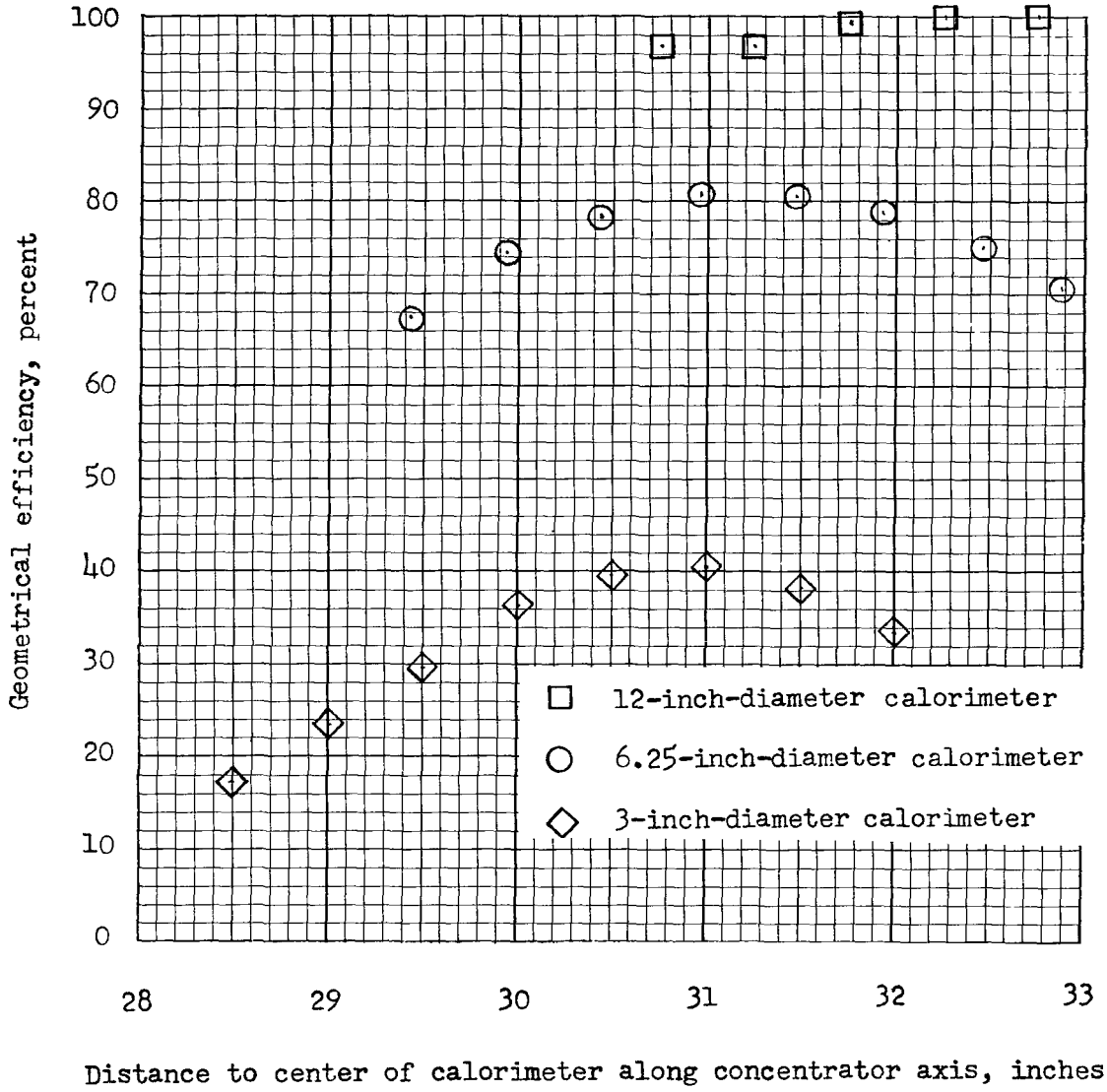

Figure 9.- Variation of geometrical efficiency with position of calorimeter along theoretical optical axis of the 10-foot-diameter split-rib concentrator.

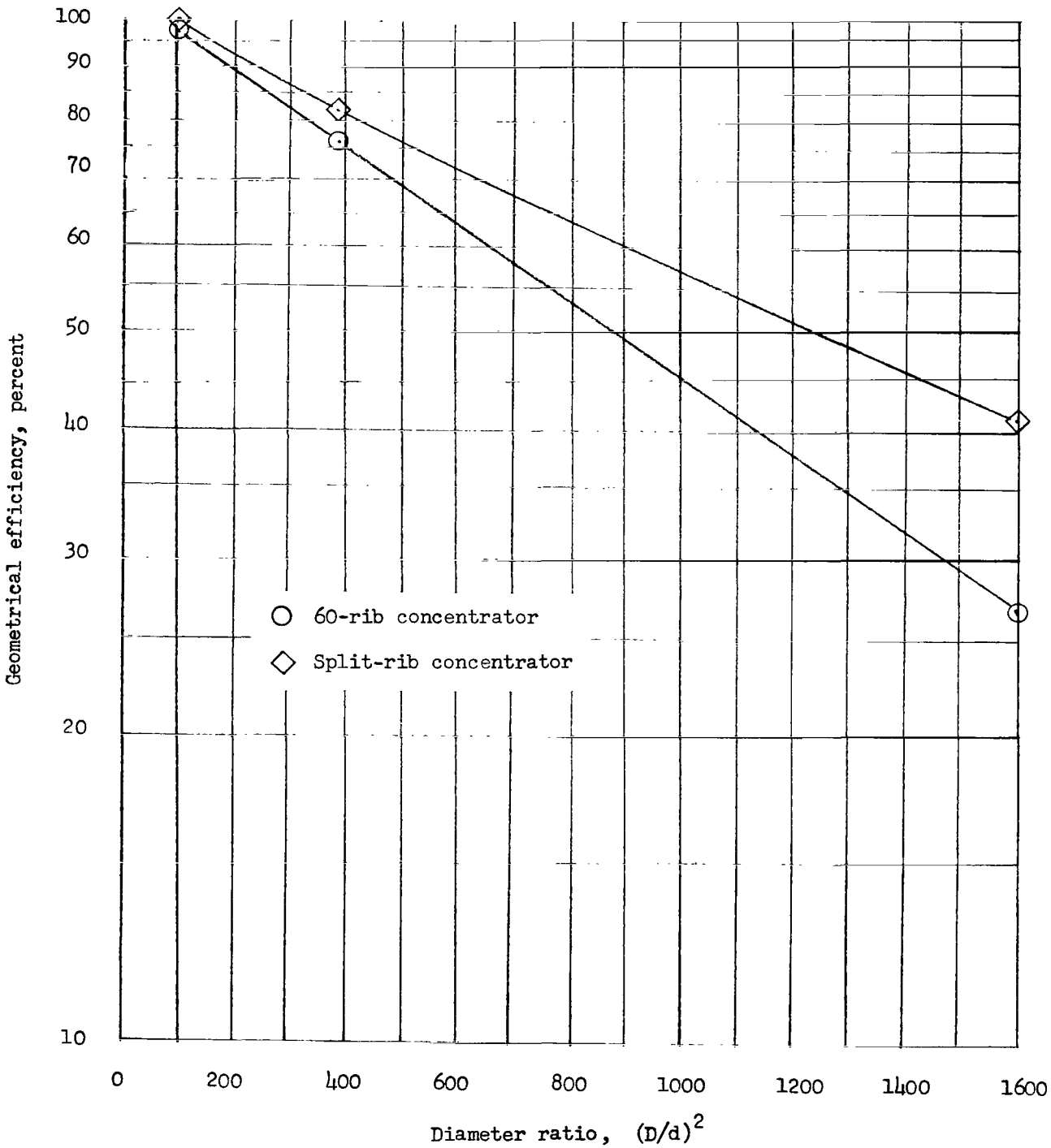

Figure 10.- Efficiency of concentrator for various diameter ratios.

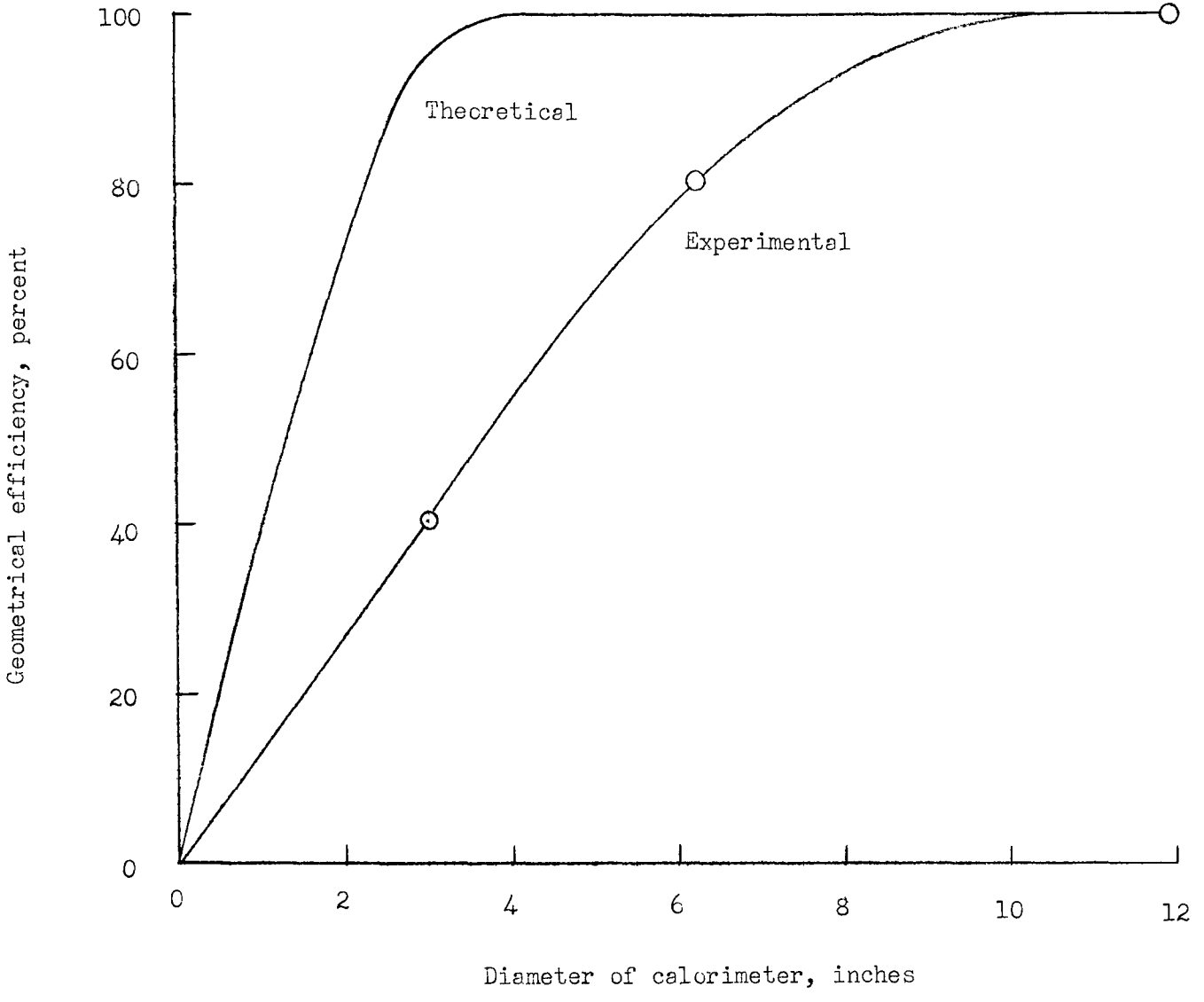

Figure 11.- Variation of geometrical efficiency with diameter of calorimeter for split-rib concentrator.

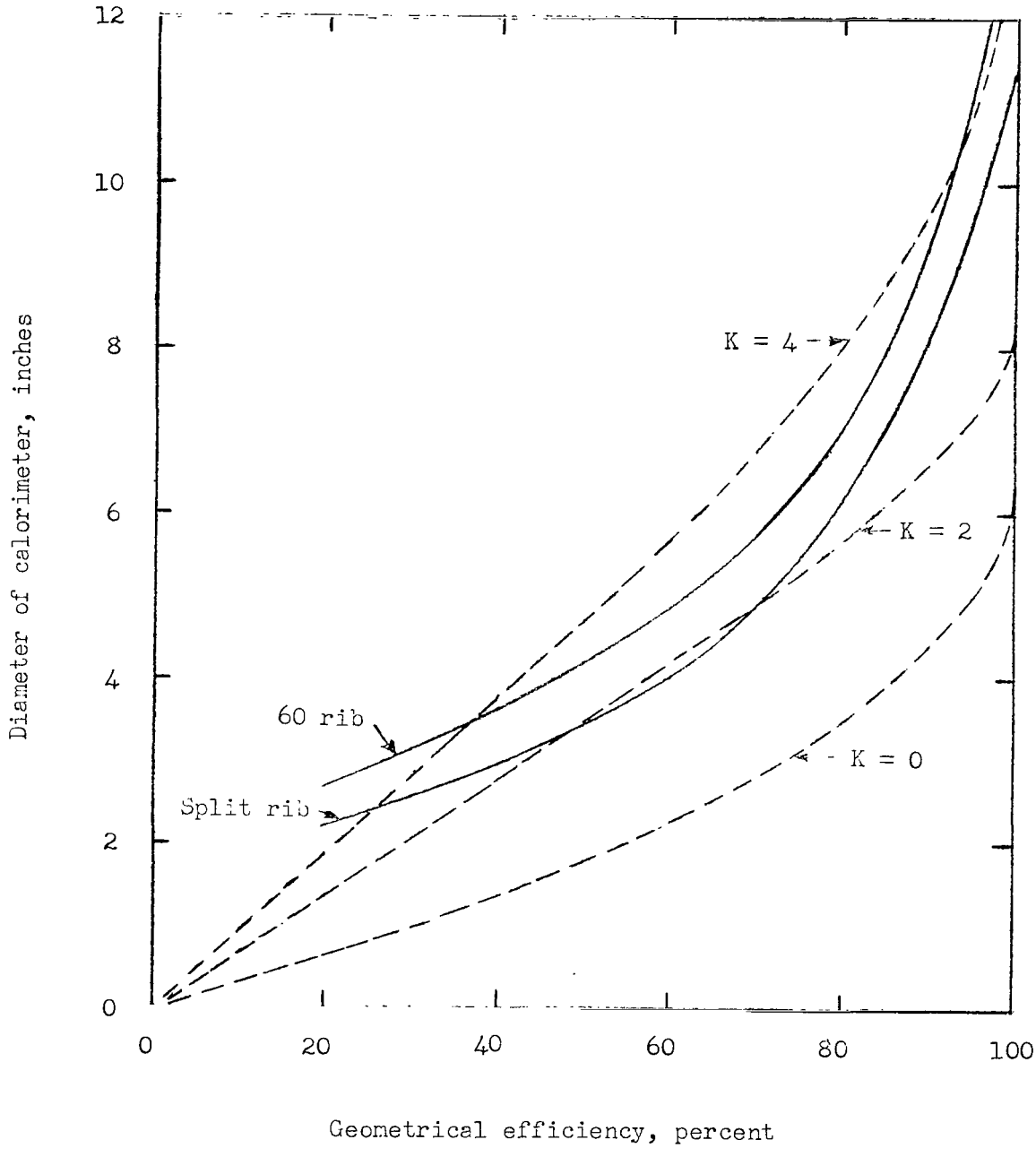

Figure 12.- Variation of geometrical efficiency with calorimeter diameter for 60-rib concentrator with 90° rim angle at different values of stress-geometry parameter K.

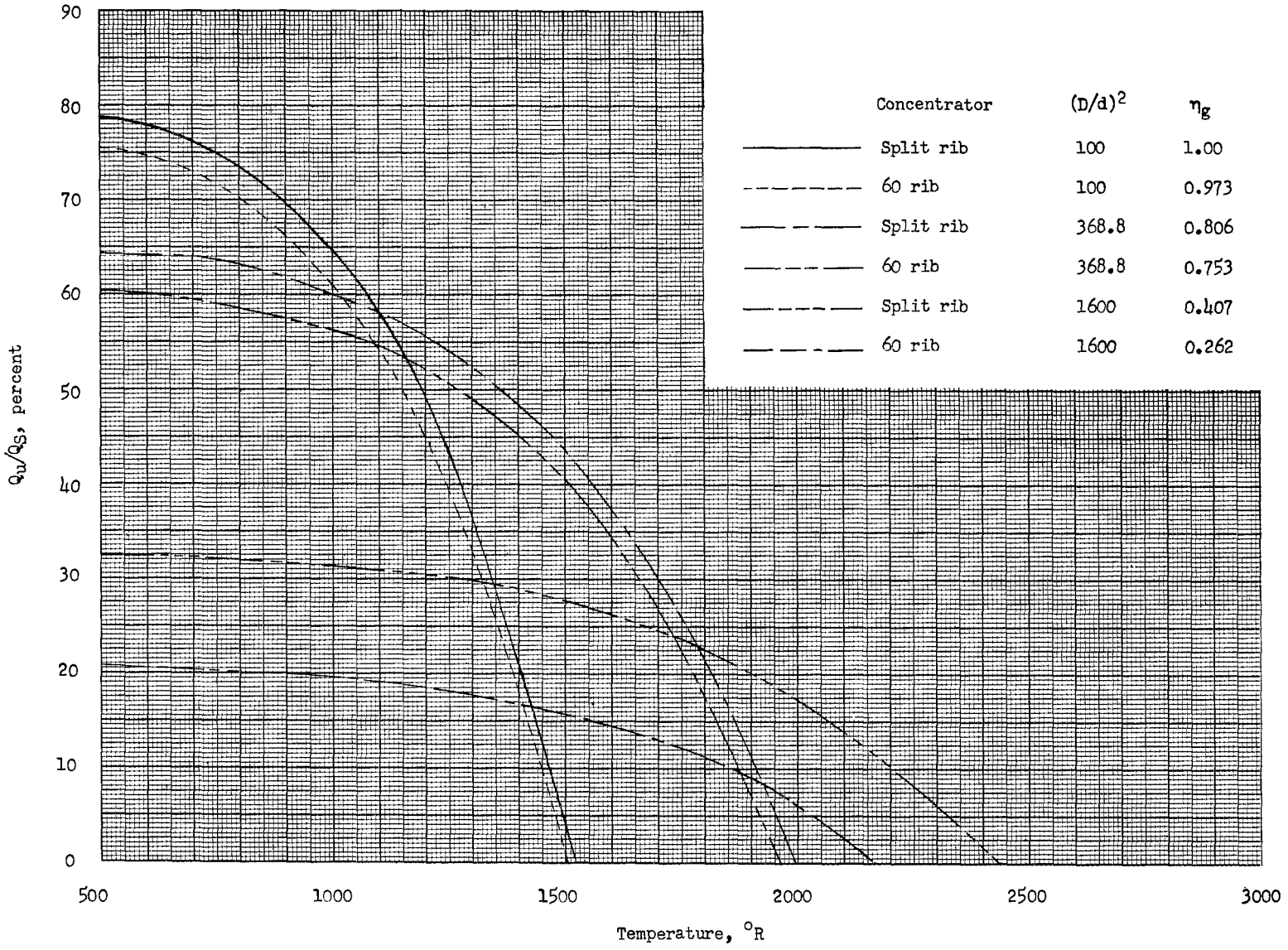

Figure 13.- Ratio of usable energy to available energy for various concentration ratios and heat receiver temperatures for the 60-rib concentrator and split-rib concentrator. $\gamma_c = 0.83$; $\alpha_b = 0.96$; $\epsilon_b = 0.96$.

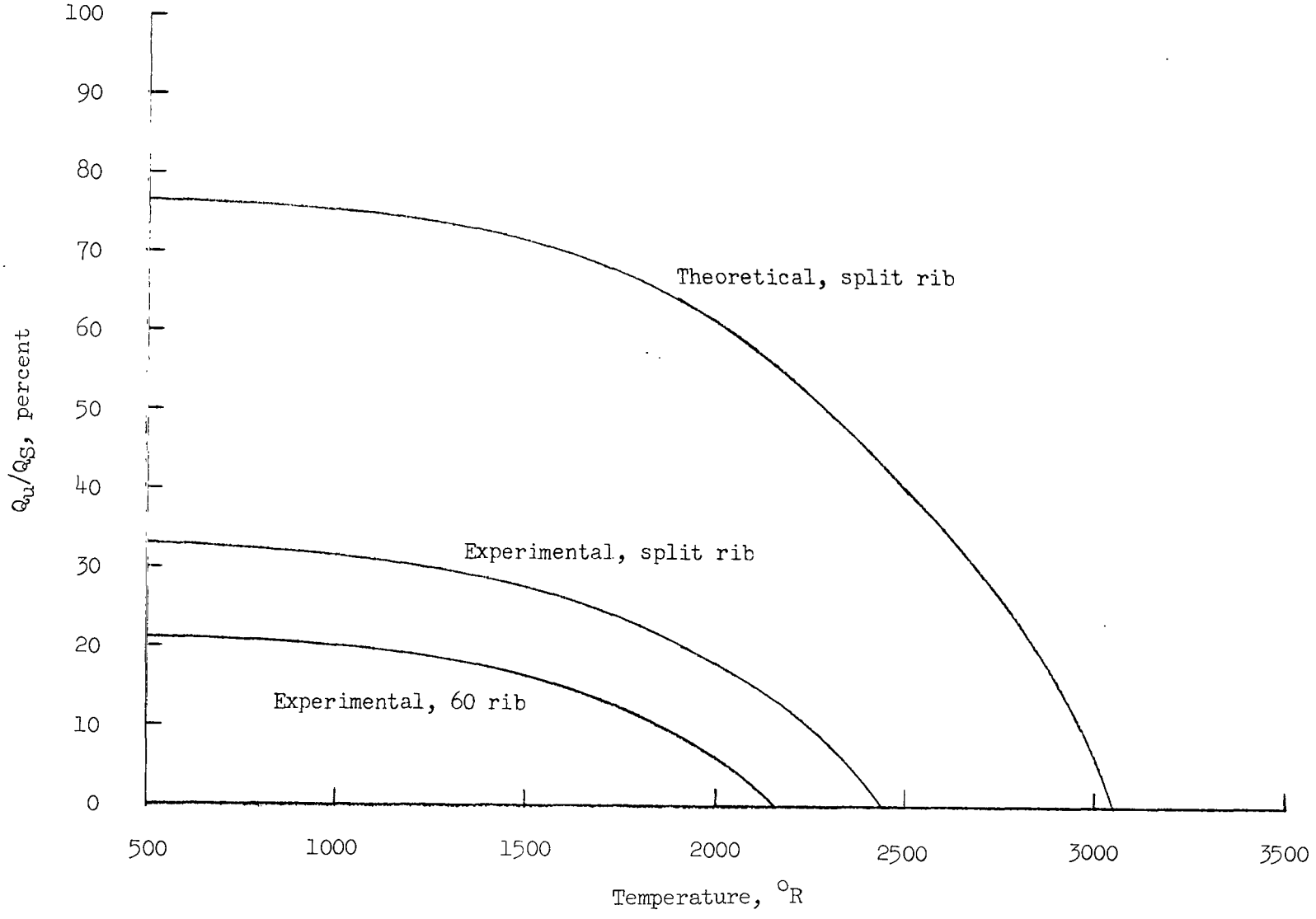

Figure 14.- Variation with temperature of ratio of usable energy to available energy for 3-inch-diameter calorimeter.